ResearchGate

See discussions, stats, and author profiles for this publication at: https://www.researchgate.net/publication/309382583

Morphology of the Insertions of the Superficial Medial Collateral Ligament and Posterior Oblique Ligament Using...

Article *in* Arthroscopy The Journal of Arthroscopic and Related Surgery · October 2016

DOI: 10.1016/j.arthro.2016.07.030

CITATIONS
0

READS
23

7 authors, including:

Goro Tajima
Iwate Medical University
17 PUBLICATIONS **310** CITATIONS

SEE PROFILE

All content following this page was uploaded by Goro Tajima on 31 October 2016.

The user has requested enhancement of the downloaded file. All in-text references underlined in blue are added to the original document and are linked to publications on ResearchGate, letting you access and read them immediately.

Morphology of the Insertions of the Superficial Medial Collateral Ligament and Posterior Oblique Ligament Using 3-Dimensional Computed Tomography: A Cadaveric Study

Takaaki Saigo, M.D., Goro Tajima, M.D., Ph.D., Shuhei Kikuchi, M.D., Jun Yan, Ph.D., Moritaka Maruyama, M.D., Ph.D., Atsushi Sugawara, M.D., Ph.D., and Minoru Doita, M.D., Ph.D.

Purpose: To describe the insertions of the superficial medial collateral ligament (sMCL) and posterior oblique ligament (POL) and their related osseous landmarks. **Methods:** Insertions of the sMCL and POL were identified and marked in 22 unpaired human cadaveric knees. The surface area, location, positional relations, and morphology of the sMCL and POL insertions and related osseous structures were analyzed on 3-dimensional images. **Results:** The femoral insertion of the POL was located 18.3 mm distal to the apex of the adductor tubercle (AT). The femoral insertion of the sMCL was located 21.1 mm distal to the AT and 9.2 mm anterior to the POL. The angle between the femoral axis and femoral insertion of the sMCL was 18.6°, and that between the femoral axis and the POL insertion was 5.1°. The anterior portions of the distal fibers of the POL were attached to the fascia cruris and semimembranosus tendon, whereas the posterior fibers were attached to the posteromedial side of the tibia directly. The tibial insertion of the POL was located just proximal and medial to the superior edge of the semimembranosus groove. The tibial insertion of the sMCL was attached firmly and widely to the tibial crest. The mean linear distances between the tibial insertion of the POL or sMCL and joint line were 5.8 and 49.6 mm, respectively. **Conclusions:** This study used 3-dimensional images to assess the insertions of the sMCL and POL and their related osseous landmarks. The AT was identified clearly as an osseous landmark of the femoral insertions of the sMCL and POL. The tibial crest and semimembranosus groove served as osseous landmarks of the tibial insertions of the sMCL and POL. **Clinical Relevance:** By showing further details of the anatomy of the knee, the described findings can assist surgeons in anatomic reconstruction of the sMCL and POL.

The superficial medial collateral ligament (sMCL) and posterior oblique ligament (POL) are the 2 main static stabilizers of the medial side of the knee.[1,2] They act as primary restraints to valgus stress and internal rotation, respectively.[3,4] Together, they are also secondary restraints to valgus, rotatory, anterior, and posterior stresses[5-8] and have a complementary relation to achieve posteromedial stability.[4,5,9-11] Thus, injuries to the sMCL and POL can result in clinically significant valgus or rotational instability.[3,12] Furthermore, dysfunction of the sMCL and POL can increase the risk of damaging associated ligamentous structures, such as native and reconstructed anterior cruciate ligaments.[8,12,13] The medial collateral ligament (MCL) is the ligamentous structure of the knee that is injured most frequently. Most MCL injuries are isolated and can be treated nonsurgically with excellent results. However, combined sMCL and POL injuries can lead to chronic instability, which causes functional limitations and osteoarthritis.[14]

Treatment of sMCL and POL injuries of the knee remains controversial. Numerous surgical methods for the repair or reconstruction of these ligaments have been reported, with recent studies showing better clinical

From the Departments of Orthopaedic Surgery (T.S., G.T., S.K., M.M., A.S., M.D.) and Anatomy (J.Y.), Iwate Medical University, Morioka, Japan.

The authors report that they have no conflicts of interest in the authorship and publication of this article.

Study supported by the Japan Society for the Promotion of Science (KAKENHI grant No. 15K01562).

Received February 10, 2016; accepted July 22, 2016.

Address correspondence to Goro Tajima, M.D., Ph.D., Department of Orthopaedic Surgery, Iwate Medical University, 19-1 Uchimaru, Morioka, Iwate 020-8505, Japan. E-mail: goro.t@triton.ocn.ne.jp

© 2016 by the Arthroscopy Association of North America

0749-8063/16112/$36.00

http://dx.doi.org/10.1016/j.arthro.2016.07.030

results with reconstruction than with repair.[15-17] An anatomic method for reconstruction of the medial knee has been shown to achieve near-normal stability.[18,19] However, a recent systematic review showed that most medial reconstruction methods are nonanatomic: On the basis of a review of 4,600 references, only 2 methods were classified as "anatomic reconstructions."[20]

Insertions of the sMCL and POL have been described in several anatomic studies, but only a few have focused on the positional relation between them and the related osseous landmarks (especially with regard to the tibial insertion of the POL).[3,19,21,22] A prerequisite for the precise repair or anatomic reconstruction of the sMCL and POL is definition of the optimal positions of those insertions and assessment of their related osseous landmarks. The aim of this study was to describe the insertions of the sMCL and POL and their related osseous landmarks. We hypothesized that these insertions and their related osseous landmarks would be consistent among individuals.

Methods

Specimen Preparation

The 22 unpaired human cadaveric knees (18 male and 4 female specimens; age range, 61-92 years; mean age, 78 years) used in this study had no severe macroscopic degenerative or traumatic changes. All cadavers had been fixed in 10% formalin and preserved in 50% alcohol for 6 months. This cadaveric study was approved by our institutional review board (H27-99). Preparation began by removing the skin and soft subcutaneous tissue on the medial side of the knee, followed by removal of the sartorius, gracilis, and semitendinosus muscles. Then, the medial retinaculum and medial patellofemoral ligament were peeled away from the sMCL and POL, which allowed the latter 2 ligaments to be identified and observed grossly. The sMCL was dissected from the tibial side. Tibial insertions of the sMCL had 2 distinct attachments located at the proximal and distal portions of the bone. However, because the proximal tibial insertion of the sMCL was merged with the deep MCL, the outline of the insertion could not be defined. The distal tibial insertion of the sMCL was broad based and attached strongly and directly to the bone. We then cut the sMCL between the proximal and distal tibial insertions and lifted it off, leaving the underlying deep MCL intact. The sMCL was attached loosely to the anterior portion of the POL and thus separated readily. Dissection of the POL from the femoral side showed that it was located superficial to the medial joint capsule in an extra-articular layer. This position allowed its release from the articular capsule. The POL was cut at its midsubstance and dissected, but the underlying capsule was left intact. The anterior portion of the POL was also dissected from the semimembranosus tendon (SM) and fascia cruris. Turning over the dissected SM revealed the tibial insertion of the POL. Insertions of the sMCL and POL were defined as the areas of the ligament fiber arising from the femur and tibia, respectively. Native insertions of both ligaments were outlined using a drill (diameter, 1.2 mm), with care taken to avoid destruction of the bone and surrounding structures.

Three-Dimensional Measurements and Visualization

Knees were imaged using a 16-row multislice computed tomography (CT) scanner (ECLOS; Hitachi Medical, Tokyo, Japan). Axial-plane images with 0.5-mm slices were obtained and saved as Digital Imaging and Communications in Medicine (DICOM) data. All digital imaging data were uploaded to dedicated software (Mimics, version 15.0, and MedCAD module; Materialise, Leuven, Belgium), and 3-dimensional (3D) images of the knee were created and referenced off the bone automatically. Then, images were used to analyze the insertion sites of the sMCL and POL as well as the related osseous structures. Insertion sites were marked and colored automatically using dedicated software. They were referenced off the bone, which was outlined by a drill during dissection. The surface area of the insertions was calculated from the 3D images using the aforementioned software, which automatically defines the center of the insertion site as the centroid of the area. Apices of the related osseous structures were determined as the furthest-protruding points, based on coronal CT images of the femur and tibia. Linear distances and angles between the center of the insertions of the sMCL and POL and the apex of the related osseous landmarks were measured on the 3D images. The accuracy of the length and area measurements was less than 0.1 mm and less than 0.1 mm^2, respectively. Comparison of the accuracy of the 3D models generated from the CT data with the optical scan showed that the mean error was 0.2 ± 0.31 mm, or approximately one-third of the pixel size.[23] The tolerance and margin of error of the CT measurements (according to the manufacturer) were ± 0.39 mm. The distribution of each variable was checked for normality using the Kolmogorov-Smirnov test. Statistical data were calculated using SPSS software (version 20.0; IBM, Armonk, NY).

We used a coordinate plane to standardize and ensure the reproducibility of the size variation of each cadaver, which had a normal distribution. A true lateral view of the femur and tibia was created based on the methods of Fujino et al.[24] and Tajima et al.[25] With the dedicated software in transparent mode ("toggle transparency"), the 3D images of the femur were set so that the posterior portions of the medial and lateral femur condyle overlapped. The 3D images of the tibia were set so that the medial and lateral aspects of the tibial plateau overlapped, after which the images were adjusted to the medial and lateral posterior tibial condyle. These images were projected onto a 2-dimensional view, and

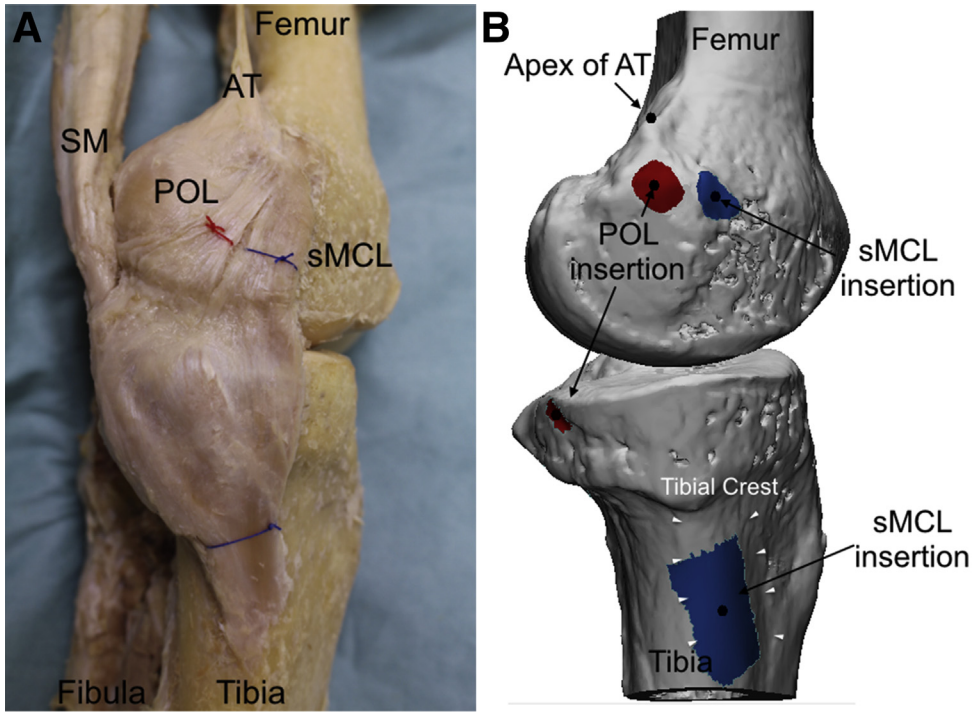

Fig 1. (A) Macroscopic findings with a medial view of the left knee showing the superficial medial collateral ligament (sMCL) (blue string), posterior oblique ligament (POL) (red string), adductor tubercle (AT), and semimembranosus tendon (SM). (B) Three-dimensional image of the medial view of the left knee showing the reconstructed insertion area of the sMCL and POL and the related osseous landmarks. The blue areas show the sMCL insertion, the red areas show the POL insertion, and the white arrowheads indicate the tibial crest.

a true lateral view was created. The coordinates of the center of the sMCL and POL insertions were mapped on squares in the true lateral view. Then, the positional relation of the insertions of the sMCL and POL and the related osseous landmarks were analyzed.

Results

Macroscopic Findings

The femoral insertion of the sMCL was located in a depression distal and anterior to the adductor tubercle (AT). The apex of the AT could be palpated readily. The medial epicondyle (ME) was palpated, but its apex was not identified clearly because it was flat or shaped like a shallow groove. The gastrocnemius tubercle (GT) was palpated as the insertion of the gastrocnemius tendon; however, its apex was also not identified clearly because of its variable and shallow shape. The femoral insertion of the POL was located posterior to the sMCL and distal to the apex of the AT. The POL runs in a "fan-like" fashion as it courses distally, with the anterior part of the distal POL fibers merging with the fascia cruris

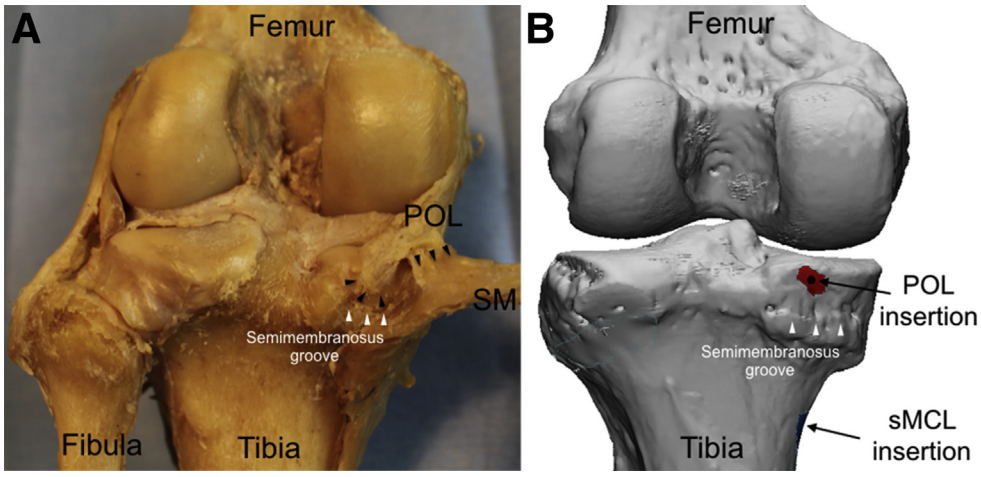

Fig 2. (A) Macroscopic findings with a posterior view of the left knee showing the posterior oblique ligament (POL) insertion and related osseous landmarks. The black arrowheads indicate the POL insertion, where it attaches to the semimembranosus tendon (SM) and tibia directly, and the white arrowheads indicate the semimembranosus groove, the bony canal to which the direct arm of the SM attaches. (B) Three-dimensional image of a posterior view of the left knee showing the reconstructed insertion area of the direct insertion of the POL (red area), as well as the semimembranosus groove (white arrowheads). (sMCL, superficial medial collateral ligament.)

Table 1. Surface Areas of Insertions of sMCL and POL Calculated Automatically on 3-Dimensional Images

	Mean Surface Area of sMCL Insertion, mm^2	Mean Surface Area of POL Insertion, mm^2
Femur	71.4 ± 18.4 (47.3-104.3)	71.5 ± 16.4 (34.9-104.5)
Tibia	266.8 ± 67.3 (187.4-410.5)	38.8 ± 14.8 (15.4-81.1)

NOTE. Data are presented as mean ± standard deviation (range).
POL, posterior oblique ligament; sMCL, superficial medial collateral ligament.

and SM. The posterior fibers were attached to the posteromedial side of the tibia directly (Figs 1 and 2). The direct tibial insertion of the POL was just above the semimembranosus groove (the bony canal to which the direct arm of the SM attaches). The semimembranosus groove was identified as the direct insertion of the SM even though it was difficult to palpate. The tibial insertion of the sMCL was firmly and widely attached to the tibial crest.

Three-Dimensional Analysis of sMCL and POL Insertions and Related Osseous Landmarks

The 3D images were used to analyze the insertions of the sMCL and POL (Figs 1 and 2). The mean surface area of the femoral and tibial insertions of the sMCL was 71.4 ± 18.4 and 266.8 ± 67.3 mm^2, respectively. The mean surface area of the femoral and tibial insertions of the POL was 71.5 ± 16.4 and 38.8 ± 14.8 mm^2, respectively (Table 1). Coordinates for the centers of the sMCL and POL insertions and the apex of the AT were obtained (Fig 3), and their locations and coordinates on a true lateral view on the 3D images were summarized (Table 2). The AT was clearly identified as an osseous landmark on the 3D images of all knees; however, the ME was not readily distinguished on the images because it was flat or appeared as a shallow groove. The femoral insertion of the POL was distal to the apex of the AT (and thus almost parallel with the long axis of the femur), and that of the sMCL was anterior to the POL. The sMCL was 8.0 ± 3.4 mm anterior and 21.3 ± 3.7 mm distal to the AT, whereas the POL was 3.0 ± 4.2 mm anterior and 18.1 ± 3.3 mm distal to the AT (Table 3). The mean linear distance between the apex of the AT and the center of the femoral insertion of the sMCL was 21.1 ± 3.0 mm, and that between the apex of the AT and center of the POL was 18.3 ± 3.2 mm. The mean linear distance between the center of the sMCL and POL femoral insertions was 9.2 ± 2.2 mm (Table 3). The angle between the line parallel to the femoral axis passing through the apex of the AT and the center of the femoral insertion of the

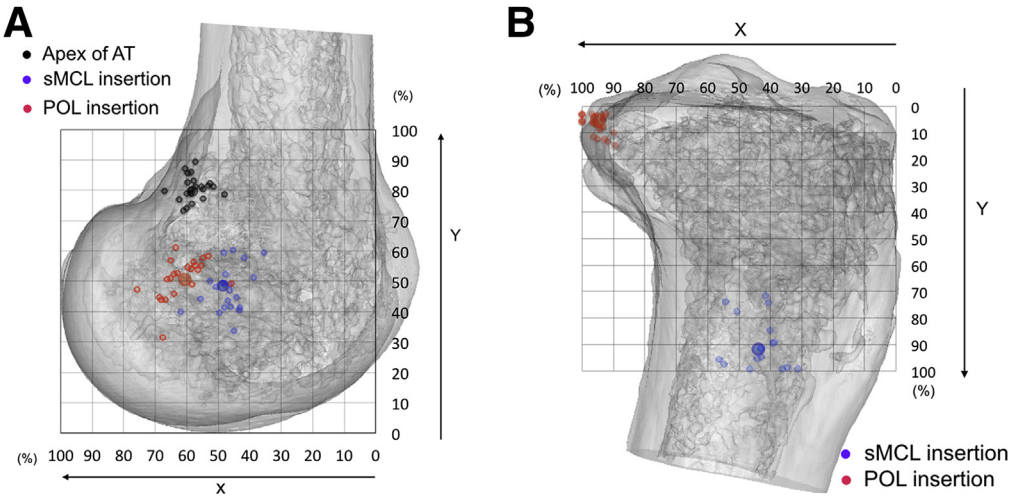

Fig 3. (A) Medial view of the femur of the left knee and an overlaying grid. A line was drawn on the true lateral view between the anterior femoral cortex and the most posterior portion of the medial condyle to serve as the standard (100%). The x-axis is the bottom of the squares, the y-axis is the distal perpendicular line on the squares, and the origin of the coordinate axes is the point of intersection of the lowest line and the distal perpendicular lines. The top of the y-axis was set the same as the standard length of the x-axis. The proximal-distal ratio is the same length as the standard x-axis (100%) because the map forms a square. Coordinates for the centers of the superficial medial collateral ligament (sMCL) insertion (blue circles) and posterior oblique ligament (POL) insertion (red circles), as well as the apex of the adductor tubercle (AT) (black circles), are shown. (B) Medial view of the tibia of the left knee and an overlaying grid. The most anterior point of the line indicates 0%, and the most posterior point, 100%. The x-axis is the bottom of the square, the y-axis is the distal perpendicular line on the squares, and the origin of the coordinate axes is the point of intersection of the highest line and the proximal perpendicular lines. The top of the y-axis was set the same as the standard length of the x-axis. The proximal-distal ratio is the same length as the standardized x-axis (100%) because this map is a square. Coordinates for the centers of the sMCL insertion (blue circles) and POL insertion (red circles) are shown.

Table 2. Locations and Coordinates of Femur and Tibia on True Lateral View on 3-Dimensional Images

	A-P Ratio (x-axis), %	P-D Ratio (y-axis), %
Center of sMCL femoral insertion	46.9 ± 5.5 (35.5-61.8)	47.5 ± 7.3 (33.8-60.3)
Center of POL femoral insertion	61.6 ± 6.6 (45.8-75.8)	51.2 ± 6.5 (31.6-61.1)
Apex of AT	57.6 ± 4.1 (48.0-66.9)	80.7 ± 4.1 (73.2-89.3)
Center of sMCL tibial insertion	43.1 ± 6.7 (31.2-56.3)	92.9 ± 10.8 (71.4-110.8)
Center of POL femoral insertion	95.5 ± 3.4 (90.0-100)	7.0 ± 3.8 (2.7-14.7)

NOTE. Data are presented as mean ± standard deviation (range).
A-P, anterior-posterior; AT, adductor tubercle; P-D, proximal-distal; POL, posterior oblique ligament; sMCL, superficial medial collateral ligament.

sMCL was 18.6° ± 11.2°. The angle between the line parallel to the femoral axis passing through the apex of the AT and the center of the POL insertion was 5.1° ± 14.7° (Table 3). The tibial insertion of the sMCL was located on the tibial crest and was positioned widely in all knees; it was 49.6 ± 5.3 mm from the joint line and 34.0 ± 5.6 mm from the anterior cortex (Table 3). The direct tibial insertion of the POL was located just proximal and medial to the superior edge of the semimembranosus groove, which was identified

Table 3. Three-Dimensional Measurements of sMCL, POL, and AT

Positional Relations	Data
Distance between sMCL femoral insertion and AT, mm	21.1 ± 3.0 (16.4-26.9)
Anterior, mm	8.0 ± 3.4 (3.5-15.5)
Posterior, mm	21.3 ± 3.7 (17.2-26.9)
Distance between POL femoral insertion and AT, mm	18.3 ± 3.2 (13.3-25.0)
Anterior, mm	3.0 ± 4.2 (−7.1 to 8.7)
Posterior, mm	18.1 ± 3.3 (14.3-24.6)
Distance between sMCL and POL femoral insertion, mm	9.2 ± 2.2 (5.1-12.6)
Angle between line Z and sMCL insertion, °	18.6 ± 11.2 (0-36)
Angle between line Z and POL insertion, °	5.1 ± 14.7 (−27 to 20)
Distance between sMCL tibial insertion and joint line, mm	49.6 ± 5.3 (39.8-59.7)
Distance between sMCL tibial insertion and anterior cortex, mm	34.0 ± 5.6 (27.5-43.1)
Distance between POL tibial insertion and joint line, mm	5.8 ± 1.6 (3.6-9.7)

NOTE. Data are presented as mean ± standard deviation (range).
AT, adductor tubercle; POL, posterior oblique ligament; sMCL, superficial medial collateral ligament.

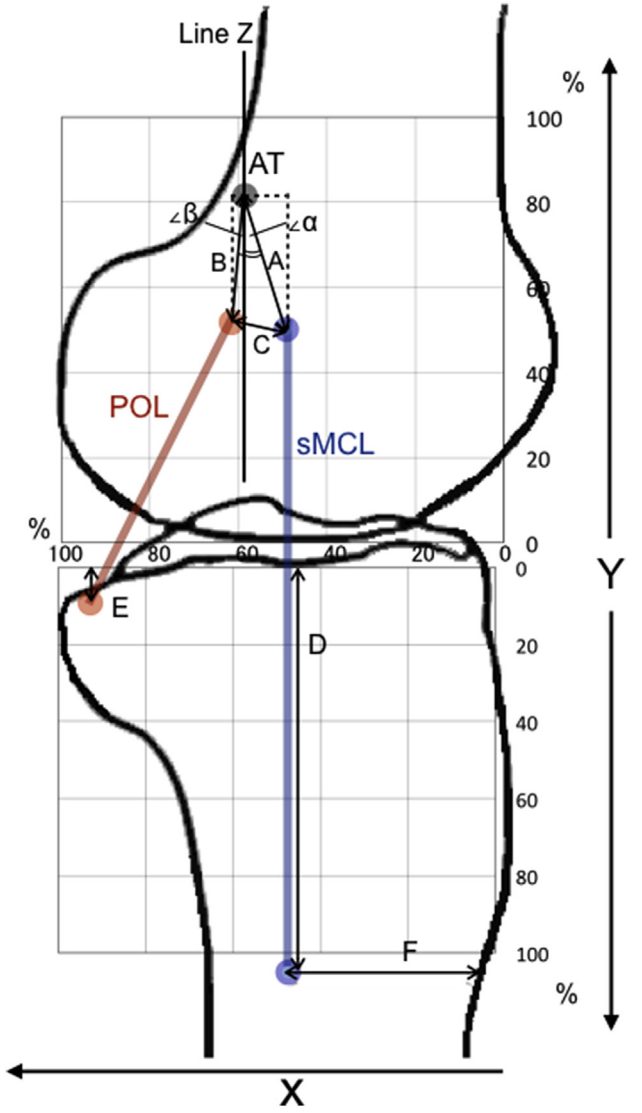

Fig 4. Summary of study results. A is the distance between the superficial medial collateral ligament (sMCL) insertion and adductor tubercle (AT); B, the distance between the posterior oblique ligament (POL) and AT; and C, the distance between the sMCL and POL. The dotted line shows the distance between the sMCL and POL insertions and the AT in the direction of the x- and y-axes. Line Z is the line parallel to the femoral axis passing through the apex of the AT; α, the angle between line Z and the sMCL insertion (in degrees); and β, the angle between line Z and the POL insertion (in degrees). D is the distance between the tibial insertion of the sMCL and the AT; E, the distance between the tibial insertion of the POL and AT; and F, the distance between the tibial insertion of the sMCL and the anterior cortex.

clearly on the 3D images of 19 of 22 knees. The semimembranosus groove of the other 3 knees was not easily resolved because the edge of the groove could not be distinguished. The mean linear distance between the direct tibial insertion of the POL and the joint line was 5.8 ± 1.6 mm (Table 3). These results are summarized in Figure 4.

Discussion

We used 3D images to identify both the insertions of the sMCL and POL and their related osseous landmarks. This information will assist surgeons in undertaking a more anatomic approach to surgery of the sMCL and POL. Our results showed that the AT, tibial crest, and semimembranosus groove serve as osseous landmarks of the insertions of the sMCL and POL.

Confirmation of the AT as an osseous landmark of the sMCL and POL at the femur was based on macroscopic findings and 3D images. LaPrade et al.[21] reported that the ME, GT, and AT are important osseous landmarks of the femoral insertions of the sMCL and POL. However, in our study, although we were able to palpate the ME and GT, their apices were not definitively identified either during dissection or on the 3D images because their shapes varied widely; in contrast, the apex of the AT was palpated readily during dissection and identified clearly on the 3D images from all knees. In their series Fujino et al.[24] also reported difficulty in clearly identifying the ME because it is flat or shallow. Thus, during a surgical procedure, the AT may be the most reliable osseous landmark at the femur.

Our study also showed the detailed positional relation between the AT and the femoral insertions of the sMCL and POL. According to a recent systematic review, most methods of medial knee reconstruction select one femoral position (except for anatomic double-bundle reconstruction). However, because the POL is anatomically and functionally distinct from the sMCL,[3,4,10,19,26-28] reconstruction grafts should be placed at distinct femoral insertions. Although anatomic double-bundle reconstructions with a 2-tunnel method have been reported,[29] only a few reports have described the intraoperative determination of the tunnel positions. LaPrade et al.[21] investigated the distance between the femoral insertions of the sMCL and POL and their related osseous landmarks, but our findings cannot be compared with theirs because their measurements were made on the structures themselves whereas we used 3D CT images. However, the differences might have arisen from identification of the apex of the AT and the centers of the insertions. An advantage of measurements made using dedicated software from 3D CT is that off-bone referencing is performed automatically. In addition, (1) the center of the insertions is identified automatically, (2) the surface calculation can be performed readily and automatically, and (3) the presence of each previously described bony landmark can be evaluated in detail from multiple orientations.[30] Thus, in our opinion, 3D CT measurement allows more accurate identification of the insertions in anatomic reconstructions of the sMCL and POL. The tunnel position of the femoral insertions of the sMCL and POL should be placed distinctly by considering the distance and the angle from the AT.

We also determined the coordinate positions of the centers of the femoral insertions of the sMCL and POL based on a true lateral view and 3D images. Wijdicks et al.[31] provided quantitative measurements of the medial knee structures and related osseous landmarks on anteroposterior and lateral radiographs. Hartshorn et al.[32] reported the radiographic landmarks for locating the femoral insertion of the sMCL. However, because their results were based on actual measurements, individual differences in the size of the bone cannot be ignored. Although there were size variations in each of the specimens used in our study, the coordinate positions had a normal distribution. Moreover, our mapping method showed the percentage of the actual length, so it minimized the influence of individual differences, whereas this is not the case when digital calipers are used. Furthermore, 3D CT data are directly and accurately translatable to intraoperative CT as a functional specification of this imaging modality. In assessing optimal tunnel positions, both the quantitative data provided in the aforementioned reports and the data obtained by our mapping method should be considered to reduce the influence of individual differences. Measurements made using the true lateral view on a 3D image will be more reproducible fluoroscopically, which will provide useful information for preoperative planning and fluoroscopic determination of the intraoperative tunnel position.

This study presented detailed insights into the surface area of the sMCL and POL insertions. Using 3D images, we determined that the mean area of the sMCL tibial insertion was much larger than that of the femoral insertion. This finding is similar to the observations of Liu et al.[22]; in their report the area of the femoral insertion was 80 $\pm$ 17.6 mm^2, and that of the tibial insertion was 349 $\pm$ 42.8 mm^2. By contrast, few studies have measured the surface areas of the POL insertions. Our measurements showed that the mean surface area of the POL tibial direct insertion was smaller than that of the femoral insertion because the distal POL fibers were attached not only to the tibia but also to the fascia cruris and SM. Therefore, grafts should be inserted in the bone tunnels but also attached to the SM for the POL and to the tibial crest broadly for the sMCL. Coobs et al.[29] and Lind et al.[33] recommended that in anatomic double-bundle reconstructions, the tunnel diameters should typically be 6 to 7 mm. On the basis of our cadaveric specimens, the surface area of the femoral insertions of the sMCL and POL, when converted into a circle, was 9 to 10 mm in diameter. Thus, covering all femoral native insertions requires a larger graft.

In this study the tibial insertion of the sMCL was located broadly over the tibial crest. Its center was 50 mm distal from the joint line and 34.0 mm away from the anterior cortex. Similar findings were reported by LaPrade et al.,[21] who showed that the tibial insertion

of the sMCL was broad based and just anterior to the posteromedial crest of the tibia. Liu et al.[22] reported that the mean distance between the center of the sMCL tibial insertion and the tibial joint line was 62 mm, which was slightly longer than the distance determined in our study. The differences might be due to individual differences in patient physique and the different measurement methods used.

It is also important to note that the tibial insertion of the POL was located on the posteromedial aspect of the tibia, which was just proximal and medial to the superior edge of the semimembranosus groove. LaPrade et al.[21] reported that the POL has 3 arms (superficial, central, and capsular), with the central arm being its main component because it reinforces the posterior joint capsule distally and attaches directly to the tibia. Although the central arm of the POL should be considered for reconstruction,[34] the positional relations of the direct tibial insertion of the POL and related osseous landmarks have not been examined in detail, and the position of the tibial insertion of the POL in reconstructive tunnels has been accordingly variable.[33,35,36] We could not distinguish the 3 arms of the POL, but our study showed the positional relation of the direct tibial insertion of the POL and the semimembranosus groove. The latter is a useful osseous landmark of the direct tibial insertion of the POL when carrying out anatomic reconstructions of the sMCL and POL.

Limitations

Our study had several limitations. First, a small number of specimens was investigated. Second, the cadaveric specimens were obtained from older individuals such that the influence of degenerative changes cannot be ruled out. Third, the sex, physique, and ethnicity of the cadavers might have influenced our results. Fourth, we did not compare CT and cadaveric measurements. Finally, despite the accuracy of the 3D measurements, the dissections were carried out by humans, such that subjective decisions may have introduced error and bias into subsequent steps.

Conclusions

This study used 3D images to show the insertions of the sMCL and POL as well as their related osseous landmarks. The AT was identified as an osseous landmark of the femoral insertions of the sMCL and POL and the tibial crest and semimembranosus groove as osseous landmarks of their tibial insertions.

Acknowledgment

The authors express their deepest appreciation to Professors Jiro Hitomi and Yoichi Sato from the Department of Anatomy, Iwate Medial University, for their continuous support of this study. They acknowledge the support and encouragement of Youichi Kamei, M.D., Ph.D., Kotaro Fujino, M.D., Ph.D., Sanjuro Takeda, M.D., Ph.D., and Hirotaka Takahashi, M.D. They also thank Mr. Masayoshi Kamata from the Department of Radiology, Iwate Medical University Hospital, for his technical assistance.

References

1. Tibor LM, Marchant MH, Taylor DC, Hardaker WT, Garrett WE, Sekiya JK. Management of medial-sided knee injuries, part 2: Posteromedial corner. *Am J Sports Med* 2011;39:1332-1340.
2. Liu H, Wang F, Kang H, Chen B, Zhang Y, Ma L. Anatomical reconstruction of the medial collateral ligament and the posterior oblique ligament of the knee. *Acta Orthop Belg* 2012;78:400-404.
3. Robinson JR, Sanchez-Ballester J, Bull AMJ, Thomas RRde W, Amis AA. The posteromedial corner revisited. *J Bone Joint Surg Br* 2004;86:674-681.
4. Griffith CJ, Wijdicks CA, Laprade RF, Armitage BM, Johansen S, Engebretsen L. Force measurements on the posterior oblique ligament and superficial medial collateral ligament proximal and distal. *Am J Sports Med* 2010;37:140-148.
5. Haimes JL, Wroble RR, Grood ES, Noyes FR. Role of the medial structures in the intact and anterior cruciate ligament-deficient knee. Limits of motion in the human knee. *Am J Sports Med* 1994;22:402-409.
6. Ritchie JR, Bergfeld JA, Kambic H, Manning T. Isolated sectioning of the medial and posteromedial capsular ligaments in the posterior cruciate ligament-deficient knee. Influence on posterior tibial translation. *Am J Sports Med* 1998;26:389-394.
7. Petersen W, Loerch S, Schanz S, Raschke M, Zantop T. The role of the posterior oblique ligament in controlling posterior tibial translation in the posterior cruciate ligament-deficient knee. *Am J Sports Med* 2007;36:495-501.
8. Wijdicks CA, Griffith CJ, Johansen S, Engebretsen L, LaPrade RF. Injuries to the medial collateral ligament and associated medial structures of the knee. *J Bone Joint Surg Am* 2010;92:1266-1280.
9. Robinson JR, Bull AMJ, Thomas RR, Amis AA. The role of the medial collateral ligament and posteromedial capsule in controlling knee laxity. *Am J Sports Med* 2006;34:1815-1823.
10. Griffith CJ, LaPrade RF, Johansen S, Armitage B, Wijdicks C, Engebretsen L. Medial knee injury: Part 1, static function of the individual components of the main medial knee structures. *Am J Sports Med* 2009;37:1762-1770.
11. Wijdicks CA, Griffith CJ, LaPrade RF, et al. Medial knee injury: Part 2, load sharing between the posterior oblique ligament and superficial medial collateral ligament. *Am J Sports Med* 2009;37:1771-1776.
12. Battaglia MJ, Lenhoff MW, Ehteshami JR, et al. Medial collateral ligament injuries and subsequent load on the anterior cruciate ligament: A biomechanical evaluation in a cadaveric model. *Am J Sports Med* 2009;37:305-311.
13. Ahn JH, Lee SH. Risk factors for knee instability after anterior cruciate ligament reconstruction. *Knee Surg Sport Traumatol Arthrosc* 2016;24:2936-2942.

14. Kannus P. Long-term results of conservatively treated medial collateral ligament injuries of the knee joint. *Clin Orthop Relat Res* 1988;(226):103-112.
15. Stannard JP, Black BS, Azbell C, Volgas DA. Posteromedial corner injury in knee dislocations. *J Knee Surg* 2012;25:429-434.
16. Benjamin Jackson J, Ferguson CM, Martin DF. Surgical treatment of chronic posteromedial instability using capsular procedures. *Sports Med Arthrosc* 2006;14:91-95.
17. Bonasia DE, Bruzzone M, Dettoni F, et al. Treatment of medial and posteromedial knee instability: Indications, techniques, and review of the results. *Iowa Orthop J* 2012;32:173-183.
18. Wijdicks CA, Ewart DT, Nuckley DJ, Johansen S, Engebretsen L, Laprade RF. Structural properties of the primary medial knee ligaments. *Am J Sports Med* 2010;38:1638-1646.
19. Sims WF, Jacobson KE. The posteromedial corner of the knee: Medial-sided injury patterns revisited. *Am J Sports Med* 2004;32:337-345.
20. DeLong JM, Waterman BR. Surgical techniques for the reconstruction of medial collateral ligament and posteromedial corner injuries of the knee: A systematic review. *Arthroscopy* 2015;31:2258-2272.e1.
21. LaPrade RF, Engebretsen AH, Ly TV, Johansen S, Wentorf FA, Engebretsen L. The anatomy of the medial part of the knee. *J Bone Joint Surg Am* 2007;89:2000-2010.
22. Liu F, Yue B, Gadikota HR, et al. Morphology of the medial collateral ligament of the knee. *J Orthop Surg Res* 2010;5:69.
23. Gelaude F, Vander Sloten J, Lauwers B. Accuracy assessment of CT-based outer surface femur meshes. *Comput Aided Surg* 2008;13:188-199.
24. Fujino K, Tajima G, Yan J, et al. Morphology of the femoral insertion site of the medial patellofemoral ligament. *Knee Surg Sport Traumatol Arthrosc* 2015;23:998-1003.
25. Tajima G, Nozaki M, Iriuchishima T, et al. Morphology of the tibial insertion of the posterior cruciate ligament. *J Bone Joint Surg Am* 2009;91:859-866.
26. Hughston JC, Eilers AF. The role of the posterior oblique ligament in repairs of acute medial (collateral) ligament tears of the knee. *J Bone Joint Surg Am* 1973;55:923-940.
27. Hughston JC. The importance of the posterior oblique ligament in repairs of acute tears of the medial ligaments in knees with and without an associated rupture of the anterior cruciate ligament. Results of long-term follow-up. *J Bone Joint Surg Am* 1994;76:1328-1344.
28. LaPrade MD, Kennedy MI, Wijdicks CA, LaPrade RF. Anatomy and biomechanics of the medial side of the knee and their surgical implications. *Sports Med Arthrosc* 2015;23:63-70.
29. Coobs BR, Wijdicks CA, Armitage BM, et al. An in vitro analysis of an anatomical medial knee reconstruction. *Am J Sports Med* 2010;38:339-347.
30. Tensho K, Shimodaira H, Aoki T, et al. Bony landmarks of the anterior cruciate ligament tibial footprint: A detailed analysis comparing 3-dimensional computed tomography images to visual and histological evaluations. *Am J Sports Med* 2014;42:1433-1440.
31. Wijdicks CA, Griffith CJ, LaPrade RF, et al. Radiographic identification of the primary medial knee structures. *J Bone Joint Surg Am* 2009;91:521-529.
32. Hartshorn T, Otarodifard K, White EA, Hatch GF III. Radiographic landmarks for locating the femoral origin of the superficial medial collateral ligament. *Am J Sports Med* 2013;41:2527-2532.
33. Lind M, Jakobsen BW, Lund B, Hansen MS, Abdallah O, Christiansen SE. Anatomical reconstruction of the medial collateral ligament and posteromedial corner of the knee in patients with chronic medial collateral ligament instability. *Am J Sports Med* 2009;37:1116-1122.
34. Menzer H, Treme G, Wascher D. Surgical treatment of medial instability of the knee. *Sports Med Arthrosc* 2015;23:77-84.
35. Kim S-J, Lee D-H, Kim T-E, Choi N-H. Concomitant reconstruction of the medial collateral and posterior oblique ligaments for medial instability of the knee. *J Bone Joint Surg Br* 2008;90:1323-1327.
36. Dong J, Wang XF, Men X, et al. Surgical treatment of acute grade III medial collateral ligament injury combined with anterior cruciate ligament injury: Anatomic ligament repair versus triangular ligament reconstruction. *Arthroscopy* 2015;31:1108-1116.

View publication stats